.

Recent results on Charm Physics from Fermilab[1] [2]

J. C. Anjos[3] and E. Cuautle[4]

Centro Brasileiro de Pesquisas Físicas, CBPF
Rua Dr. Xavier Sigaud 150, 22290-180 Rio de Janeiro Brazil

Abstract. New high statistics, high resolution fixed target experiments producing 10^5 - 10^6 fully reconstructed charm particles are allowing a detailed study of the charm sector. Recent results on charm quark production from Fermilab fixed target experiments E-791, SELEX and FOCUS are presented.

INTRODUCTION

This review contains recent results from three Fermilab fixed target experiments dedicated to study charm physics: E791 and E871 (SELEX) of charm hadroproduction and E831 (FOCUS) of charm photoproduction.
The experiment E791 used a 500 GeV/c π^- beam incident on platinum and diamond target foils and took data in 1991-1992. A loose transverse energy trigger was used to record 2^{10} interactions. Silicon microstrip detectors (6 in the beam and 17 downstream of the target) provided precision track and vertex reconstruction. The precise location of production and decay vertices of long lived charm particles allowed to reconstruct over 2^5 charm particles.
SELEX used a 600 GeV hyperon beam of negative polarity to make a mixed beam of Σ^- and π^- in roughly equal numbers. The positive beam was composed of 92 % of protons, and 8 % of π^+. Interactions occurred in a segmented target of 5 foils, 2 Cu and 3 C. The experiment was designed to study charm production in the forward hemisphere, with good mass and decay vertex resolution for charm momenta in the range 100-500 GeV/c. A major innovation was the use of online selection criteria to identify events that had evidence for a secondary vertex. Data taking finished in 1997.
The FOCUS experiment used a photon beam with $< E_\gamma >= 170$ GeV on a Beryllium Oxide segmented target. Sucessor of Fermilab E687, FOCUS had upgrades

[1] This work is partially supported by CLAF/CNPq Brazil and CONACyT México
[2] To appear, Proc. *VII Mexican Workshop on Particles and Fields*, Merida Yuc. Méx., Nov.1999
[3] janjos@lafex.cbpf.br
[4] ecuautle@lafex.cbpf.br

in vertexing, Cerenkov identification, electromagnetic calorimetry and muon identification. The target segmentation and the use of additional silicon microstrip detectors after each pair of target segments were major improvements. The experiment took data in 1996-1997 and collected over 7 billion triggers of charm candidates. FOCUS has the largest charm sample available in the world, with over 10^6 fully reconstructed charmed particles.

The data available from these three experiments will allow to make high precision charm physics, to study rare decays and to search for new physics.

CHARM PRODUCTION AND CROSS SECTIONS FOR D MESONS

Charm production is a combination of short and long range processes. Perturbative Quantum Chromodynamics (pQCD) can be used to calculate the parton cross section, the short range process. The long range process of parton hadronization has to be modeled from experimental data. The two processes occur at different time scales and should not affect each other, leading to factorization properties. The general expression for production of charm in hadroproductions is [1]

$$\sigma(P_A, P_B) = \sum_{i,j} \int dx_A dx_B f_i^A(x_A, \mu) f_j^B(x_B, \mu) \hat{\sigma}_{i,j}(\alpha_s(\mu), x_A P_A, x_B P_B) \qquad (1)$$

where $f_i^A(x_A, \mu)$ is the probability of finding parton type i inside the hadron A with momentum fraction x_A, and μ is the scale at which the process occurs. The other hadron taking part in the interaction has $f_j^B(x_B, \mu)$. The elementary parton cross section $\hat{\sigma}_{i,j}(\alpha_s(\mu), x_A P_A, x_B P_B)$ term is calculated by QCD, according to parton models. Although QCD is well defined theory, solutions to most problems are quite difficult. So, to calculate the parton cross section we usually do a perturbative series expansion in terms of the strong interaction coupling constant, α_s, and calculate at leading order (LO), next-to-leading order (NLO) and so on. Nowadays most calculations include NLO. Some Feynman diagrams for hadroproduction of charm at LO and NLO are shown in Fig.1 (more details can be found in reference [1]).
Usually the differential cross sections is measured as a function of the scaled longitudinal momentum (Feynman x_F) $d\sigma/dx_F$, and as a function of the transverse momentum squared $d\sigma/dp_t^2$. A phenomenological parametrization of the double differential cross section often used to describe the experimental data is given by,

$$\frac{d\sigma}{dx_F dp_t^2} = A\,(1 - x_F)^n\, exp(-bp_t^2) \qquad (2)$$

where A , n and b are parameters used to fit the data. In fact kinematic considerations provide predictions for the power n at high x_F and QCD calculations give average p_t values comparable to the charm quark mass.

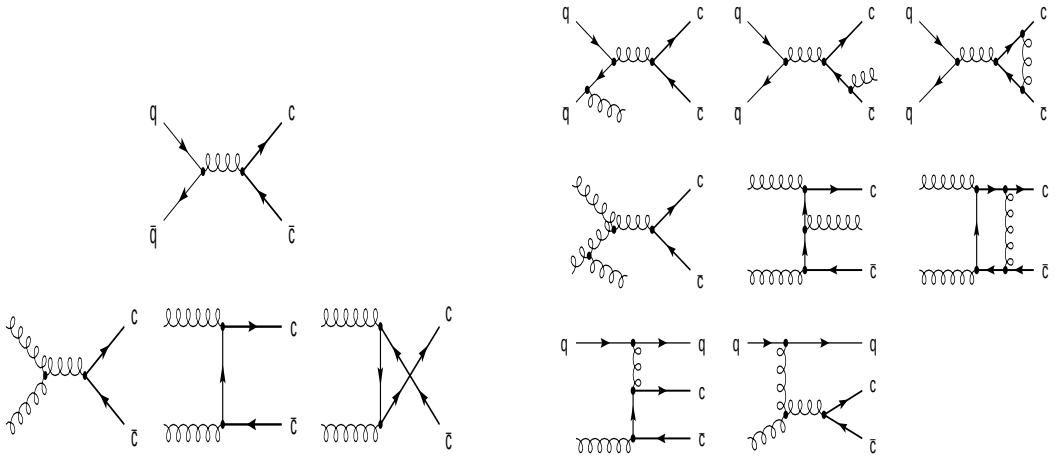

FIGURE 1. Some of Feynman diagrams for charm hadroproduction: leading order (left) and Next-to-Leading Order (right side)

E791 has measured the total forward cross section and the differential cross sections as functions of x_F and p_t^2 from a sample of 88990 ± 460 D^0 mesons. Fig. 2 shows the differential distributions and its comparison to theoretical predictions from QCD calculations at NLO [2] and to the Monte Carlo event generator, Pythia/Jetset [3] for $c\bar{c}$ and $D\bar{D}$ production. Hadron distributions are softer than $c\bar{c}$ distributions due to fragmentation. With suitable choice for the intrinsic transverse momentum k_t of the incoming partons ($k_t = 1$ GeV/c), the Peterson fragmentation function parameter ($\varepsilon = 0.01$), and the charm quark mass $m_c = 1.5$ GeV/c^2, NLO D meson calculation provides a good match to the p_t^2 distribution and fair match to the x_F distribution. The hadronization scheme implemented in Pythia/Jetset can be adjusted to fit the data. The large number of D^0 events make it possible to clearly observe a turnover point greater than zero ($x_c = 0.0131 \pm 0.0038$) in the x_F distribution. The positive value provide evidence that the gluon distribution in the pion is harder than the gluon distribution in the nucleon [4]. The total forward neutral D meson cross section measured by E791 is $\sigma(x_F > 0) = 15.4 \pm^{1.8}_{2.3}$ μb/nucleon.
SELEX has also preliminary data on D^0 cross section. Fig. 2 (right) shows the x_F distribution for D^0 + c.c. from E791 [4] and the preliminary data from SELEX. Up to $x_F = 0.5$ data overlap and agree well. However SELEX has no strong evidence for rise at large x_F as seen in the E791 data. The continuous line is a fit to the data points with the phenomenological parametrization in Eq. 2.

Correlations in the production of Charm pairs

Observation of both of the charm particles in a hadron-produced event can give additional information on the production process and allow to test QCD predic-

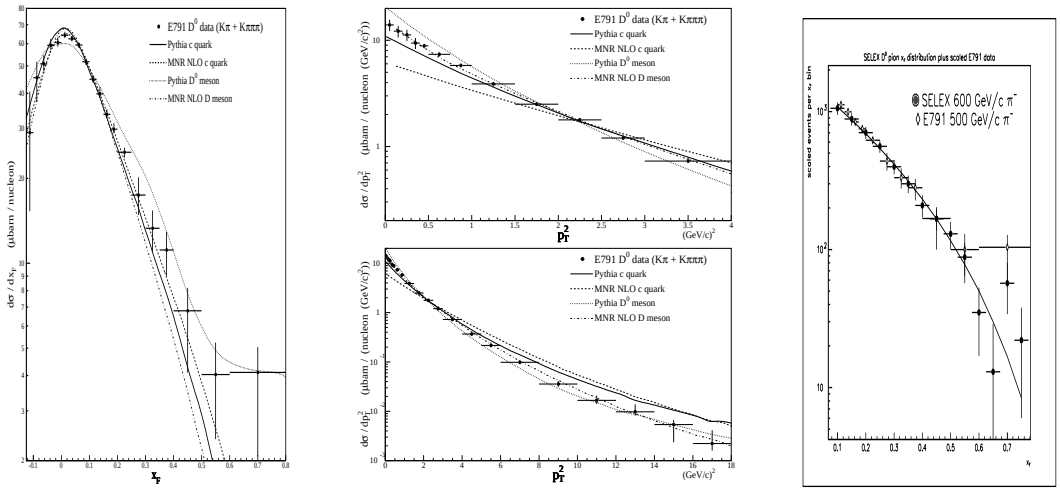

FIGURE 2. D^0 production: from E791 compared with theoretical models as a function of x_F (left), p_t^2 (central column) and compared with preliminary results from SELEX (right).

tions since both longitudinal and transverse momenta of the charm particles and angular correlations are explicitly measured.

In the simplest parton model the charm and anticharm particles are expected to be produced in opposite directions in the transverse plane. However if one assumes that the incoming partons have an intrinsic transverse momentum, k_t, this will affect the transverse momentum of the heavy quark pair, its azymuthal correlations and the transverse distribution of a single quark. The partons entering the hard interaction are indeed supposed to have a non vanishing primordial k_t, seen as a nonperturbative Fermi motion of partons inside the incoming hadrons. Typical values of k_t should thus be 300-400 MeV. However it has been noted [5] that much higher values of k_t are required, at or above 1 GeV, to reproduce charm data. This could be an indications of the importance of next to leading and higher order effects, by which emitted gluons would further modify the nearly back-to-back [6] production of the final charm hadrons.

E791 has measured correlations between D and $\bar{D}$ mesons from 791 ± 44 fully reconstructed charm meson pairs [7]. The main variables used to describe charm pair correlations are the beam direction, p_t, and either the rapidity y or the Feynman scaling variable x_F, and also the azymuthal distribution ϕ. The same way the difference and sum between these variables for two charm mesons $(D, \bar{D})$ Δx_F, Σx_F and so on.

The measured distributions are compared to predictions of the fully differential NLO calculation for $c\bar{c}$ production [2], as well as to predictions from the Pythia/Jetset Monte Carlo event generator for $c\bar{c}$ and $D\bar{D}$ production. Default parameter have been used for the theoretical models.

For the single charm distributions shown in Fig.3, we observe that for the longitudinal momentum distributions x_F and y the experimental results and theoretical predictions do not agree. In this comparison the experimental distributions are most similar to the NLO and Pythia/Jetset $c\bar{c}$ distributions, but are narrower than all three theoretical predictions. The experimental p_t^2 distribution agrees quite well with all three theoretical distributions. As expected, both the theoretical and experimental ϕ distributions are consistent with being flat.

The experimental and theoretical longitudinal distributions for pairs Δx_F , Σx_F, Δy and Σy are shown in Fig. 4. As with the single-charm distributions, the experimental results are much closer to the two $c\bar{c}$ predictions than to the Pythia/Jetset $D\bar{D}$ predictions, but narrower than all three theoretical predictions. For the transverse distributions for charm pairs any observed discrepancy between data and theory must derive from the theory modeling the correlations between the transverse momentum of the two D mesons $p_{t,D}$ and $p_{t,\bar{D}}$ because the single charm p_t^2 and ϕ experimental distributions agree well with the theory. The $\Delta\phi$ distribution shows clear evidence of correlations (more details can be found in reference [7]).

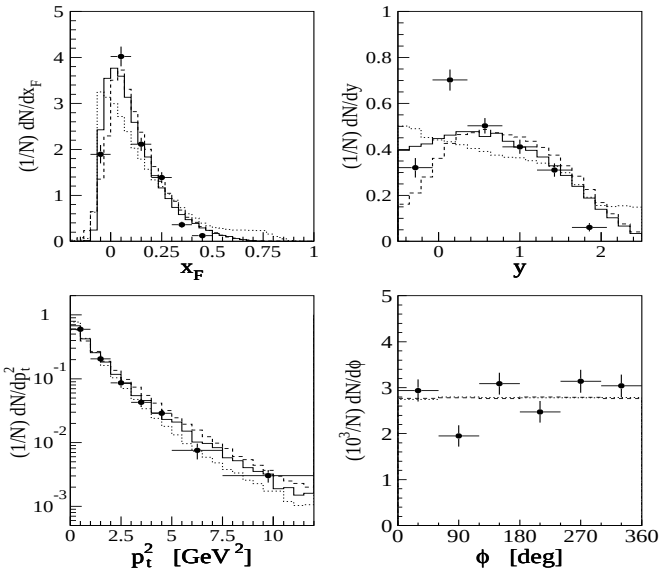

FIGURE 3. Single-charm distributions for x_F, y, p_t^2 and ϕ: weighted data (•) NLO QCD prediction (——); PYTHIA/JETSET charm quark prediction (– – – –); and PYTHIA/JETSET D meson prediction (·····). All distributions are obtained by summing the charm and anticharm distributions from charm-pair events.

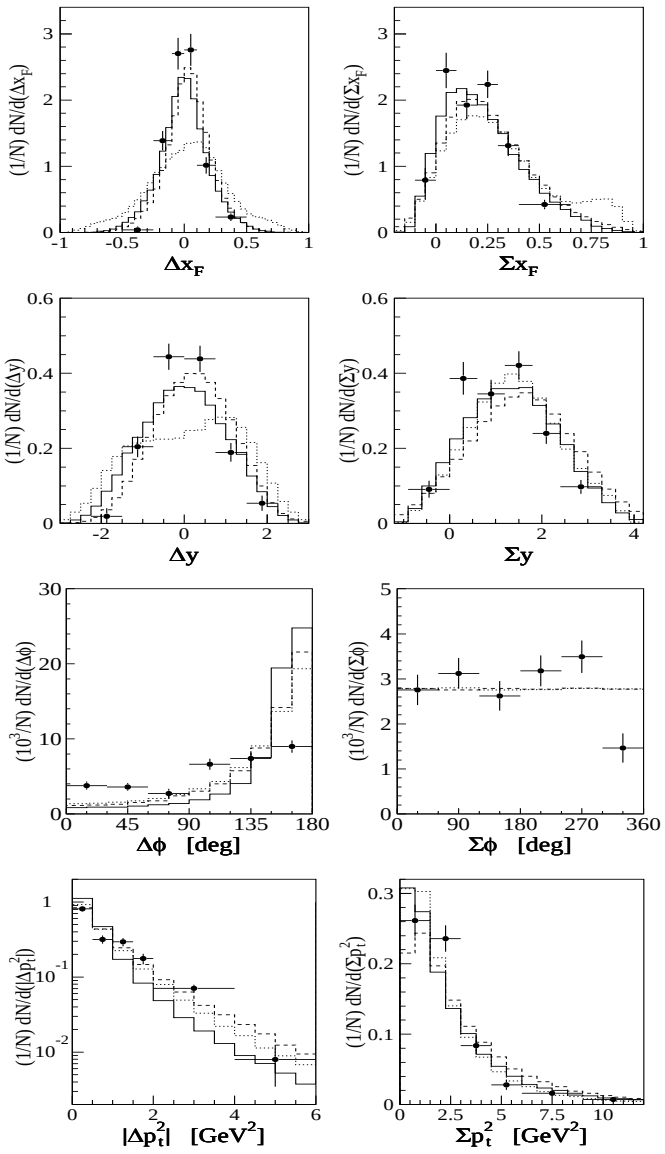

FIGURE 4. Charm-pair Δx_F, Σx_F, Δy, Σy, $\Delta\phi$, $\Sigma\phi$, Δp_t^2 and Σp_t^2 distributions; weighted data (•); NLO QCD prediction (——); PYTHIA/JETSET charm quark prediction (– – – –); and PYTHIA/JETSET D meson prediction (·····).

HADRONIZATION AND PARTICLE - ANTIPARTICLE ASYMMETRIES

The production of a charm hadron can be subdivided in two steps: the production of a $c\bar{c}$ pair followed by the hadronization of these quarks. In perturbative QCD, that describes the $c\bar{c}$ production, the x_F spectra of produced charm/anticharm quarks are identical to leading order and the effects of higher orders are very small

in this respect. Therefore any asymmetry between charm and anticharm hadrons is a simple measure of nonperturbative effects coming from the hadronization process. Particle - antiparticle asymmetries can be quantified by means of the asymmetry parameter

$$A = \frac{N - \bar{N}}{N + \bar{N}} \tag{3}$$

where N ($\bar{N}$) is the number of produced particles (antiparticles). This parameter is usually measured as a function of x_F and p_t^2.

Several experiments have reported an enhancement in the production rate of charm particles having valence quarks in common with the incident particles, relative to charge conjugate particles which have fewer or no common valence quarks. This effect is known as leading particle effect. Measurements of the asymmetry parameter A can put in evidence leading particle effects, as well as other effects like associated production of a meson and a baryon.

From the theoretical point of view, models which can account for the presence of leading particle effects use some kind of non-perturbative mechanism for hadronization, in addition to the perturbative production of charm quarks. Two examples are:

String fragmentation [8]: in this case the parton of the hard interaction and the beam remnants are connected by a string which reflect the confining color field. Successive breaking of the color flux tube stretched between a cluster, when it is kinematic possible, will create light quark-antiquark and hadrons will be produced.

Intrinsic charm model [9]: a virtual $c\bar{c}$ pair pops from the sea of the beam particle. The $c\bar{c}$ pair coalesce with the neighbor valence quarks due to their similar rapidity. This mechanism favors the production of charm particles with valence quarks in common with the beam particle at high x_F and low p_t region. A similar argument can be drawn with respect to the target.

New results on the asymmetry parameter A and evidence for leading particle effects in both meson and baryon production are available from experiments E791, SELEX and FOCUS.

E791 has measured recently the asymmetries of $D_s^{\pm}$ mesons [12]. Fig. 5 shows the $D_s^{\pm}$ asymmetry as a function of x_F and p_t^2, compared with previous $D^{\pm}$ results from the same experiment [13].

Preliminary results of $D^0(\bar{D^0})$ as well as $D^{\pm}$ asymmetries as a function of x_F presented by SELEX [10] are shown in Fig. 6 (left), for different incident beam particles (π^-, Σ^-, p). The π^- data is compared to $D^{\pm}$ asymmetries from E791. The asymmetry at $x_F > 0.4$ does not rise steeply with x_F as previously reported by E791, Fig. 6 (right).

For baryons there are also preliminary results for the asymmetry parameter. Fig.7 (left) shows the E791 results for the Λ_c^+ asymmetries as function of x_F and p_t^2, compared with predictions from Pythia/Jetset (full lines) [11]. The results show

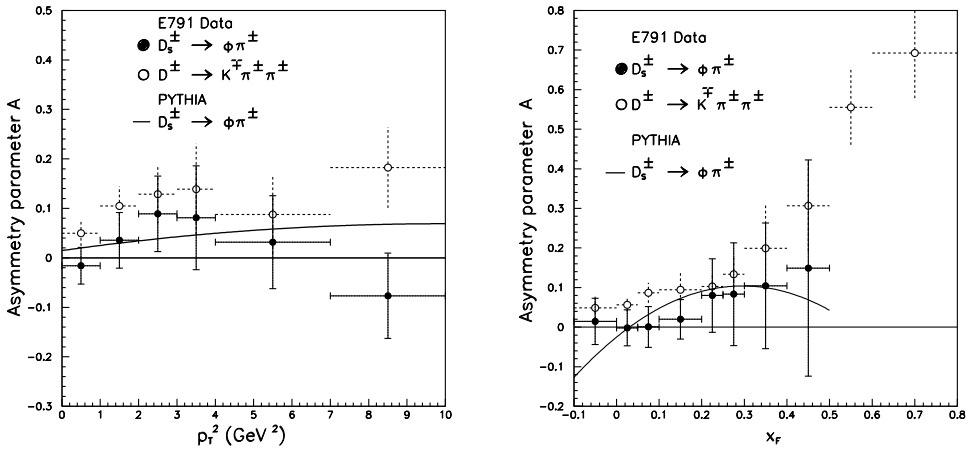

FIGURE 5. Asymmetries of D_s as a function of x_F and P_t^2, compared with $D^\pm$.

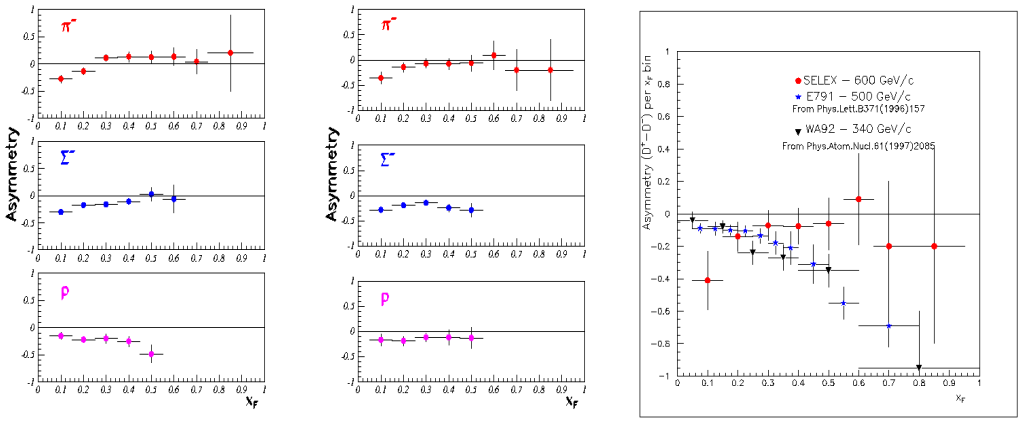

FIGURE 6. Asymmetries of D mesons from SELEX (preliminary results) and E791. The first and second columns are $D^0(\bar{D}^0)$ and $D^\pm$ asymmetries from SELEX. The right figure shows the comparison of $D^\pm$ asymmetries from SELEX and E791.

a uniform positive asymmetry of $12.7 \pm 3.4\%$ over the studied kinematical range but do not exclude a rise in the $x_F < 0$ region as predicted by Pythia/Jetset. For $x_F > 0$ the observed asymmetry does not agree with Pythia/Jetset predictions. SELEX has also measured the Λ_C^+ asymmetry as a function of x_F for different

incident beam particles (π^-, Σ^-, p) Fig. 7 (right) [10]. The asymmetry is clearly larger for the baryon beams than for the π beam. For the protons the only region in which there is $\bar{\Lambda}_c$ production is at very small x_F. Their preliminary results for the π^- beam are compatible with those from E791, Fig. 7 (left).

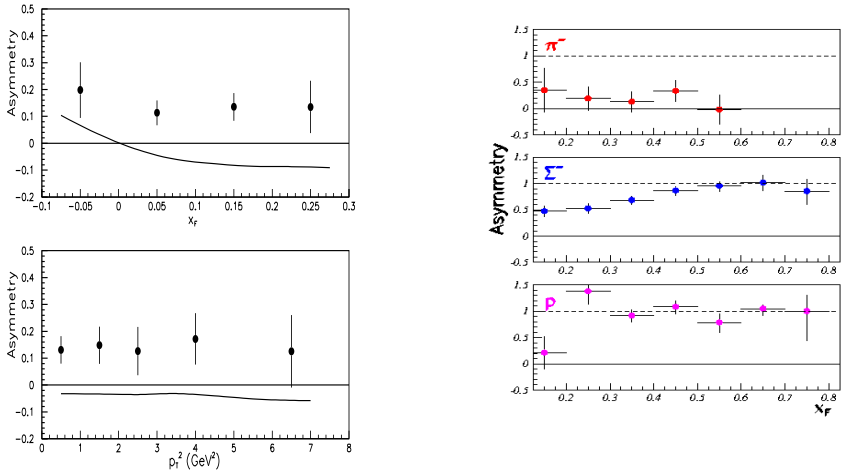

FIGURE 7. Λ_c asymmetries as function of p_t^2 and x_F from E791 (left). Λ_c asymmetries (preliminary results) as function of x_F for different beams (π^-, Σ^-, p) from SELEX (right).

FOCUS has also preliminary results on baryon asymmetries. In Fig.8 we see the Λ_c asymmetry as functions of p_l, p_t^2 and x_F obtained from a sample of about 16,000 $\Lambda_c's$, compared with Pythia/Jetset Predictions. As FOCUS has a photon beam, no leading particle effect is expected in the $x_F > 0$ region. In this case the positive asymmetry observed in all the x_F range can be an indication of charm baryon and charm meson associated production, favouring a positive asymmetry.
The high statistic Λ_c sample from FOCUS allowed to obtain about 600 $\Sigma_c \to \Lambda_c\pi$. It is interesting to compare the asymmetry for charm particles with different light quark content. We present in Fig.9 (right) very preliminary results from FOCUS comparing the $\Sigma_c^{++}(uuc)$ and $\Sigma_c^0(ddc)$ to the $\Lambda_c^+(udc)$ total asymmetry.
In Fig. 9 (left) we show the comparison between the Λ^0 and the Λ_c asymmetries as a function of x_F from E791. Their similarity suggests that the ud diquark shared by the produced Λ^0 (Λ_c^+) and nucleons in the target should play an important role in the measured asymmetry in the $x_F < 0$ region. However, one expects that Λ_c asymmetry grows more slowly than the Λ^0 asymmetry due to its higher mass.

Leading particle effects were also seen by E791 in hyperon production. Preliminary results on Λ, Ξ and Ω asymmetries as a function of x_F and p_t^2 are shown in Fig.10 in comparison with predictions from Pythia/Jetset. The range of x_F covered

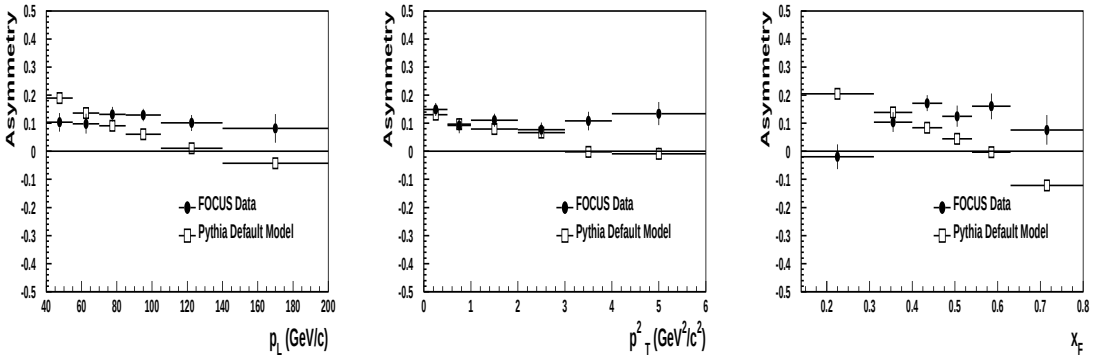

FIGURE 8. Λ_c^+ asymmetry from FOCUS as a function of p_l, p_t^2 and x_F (preliminary results), compared with Pythia/Jetset predictions

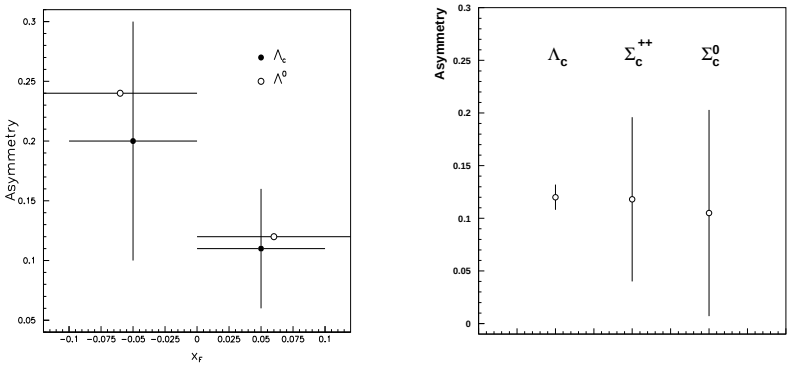

FIGURE 9. Comparison between Λ^0 and Λ_c asymmetries from E791 (left). Λ_c, Σ^{++} and Σ_c^0 total asimmetries (preliminary) from FOCUS (right).

allowed the first simultaneous study of the asymmetry in both the negative and positive x_F regions. We can clearly see leading particle effects associated with the target or with the beam particles which qualitatively agree with expectations from recombination models (see table 1) [14]. It is interesting to observe, as expected, the crossover of the Ξ asymmetry with respect to the Λ asymmetry at $x_F \simeq 0$. The positive asymmetry measured in regions $x_F > 0$ for the $\Lambda(udc)$ and for the $\Omega(sss)$ suggest the associated production of a hyperon and a kaon due to the higher energy threshold imposed by baryon number conservation for the production of an anti-hyperon. Pythia/Jetset does not reproduce the data.

TABLE 1. Hyperon asymmetries predictions

	$x_f < 0$ target(uud or ddu)	$x_f > 0$ beam π^- $(\bar{u}d)$
$\Lambda^0(uds)$	double leading	leading
$\overline{\Lambda}^0(\bar{u}\bar{d}\bar{s})$	non leading	leading
$\Xi^-(dss)$	leading	leading
$\overline{\Xi}^+(\bar{d}\bar{s}\bar{s})$	non leading	non leading
$\Omega^-(sss)$	non leading	non leading
$\overline{\Omega}^+(\bar{s}\bar{s}\bar{s})$	non leading	non leading
Recomb. Models[a]:	$A_\Lambda > A_\Xi > A_\Omega$	$A_\Xi > A_\Lambda \sim A_\Omega$

[a] Presented in Second Latin American Symposium [14]

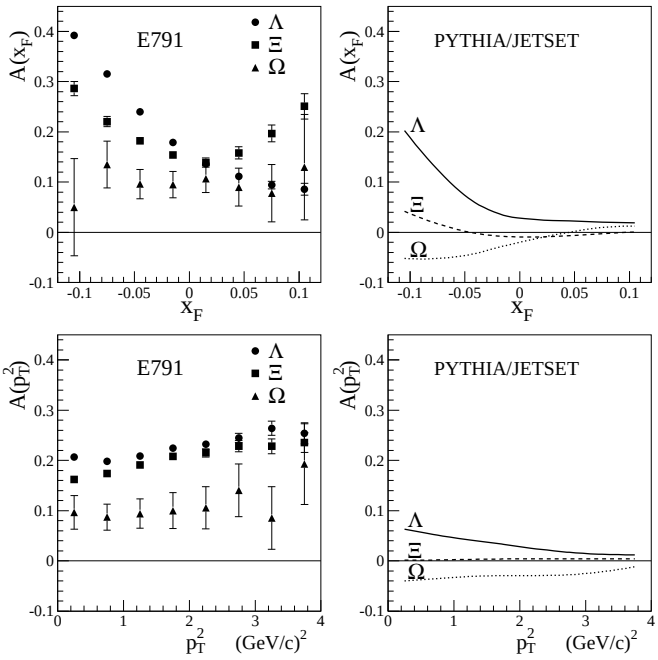

FIGURE 10. Hyperon asymmetries as a function of x_F (top) and p_T^2 (bottom) from E791 (preliminary results). The asymmetry for x_F (p_T^2) is integrated over all the p_T^2 (x_F) range of the data set. The right column show the predictions of Pythia/Jetset both as a function of x_F and p_T^2 (preliminary results).

DOUBLE CABIBBO SUPPRESSED DECAYS

The Cabibbo suppressed charm decays can provide useful insights into the weak interaction mechanism for nonleptonic decays. The $D^+ \to K^+\pi^-\pi^+$ signal obtained from 100 % of FOCUS data set consist of $\sim$ 300 events and is at least a factor of five larger than two previous observations by E687 and E791 (E791 observed 59 ± 13 events [15]). The preliminary branching ratio relative to $K^-\pi^+\pi^-$

is (0.72 ± 0.09) %, completely consistent with the world average of (0.68 ± 0.15)% and the E791 values of $(0.77 \pm 0.17 \pm 0.08)$%. We note that this is $\sim 3tan^4(\theta_c)$, which is roughly the ratio of the D^+/D^0 lifetime, indicating that the destructive Pauli interference present in the Cabibbo Favored D^+ decay is absent in the doubly Cabibbo suppressed (DCS) mode.
$D^+ \to K^-K^+K^+$ is an interesting DCS decay, which cannot even occur through a spectator diagram. FOCUS has the first observation of this mode, and reports a preliminary result for the Branching Ratio relative to $K^-\pi^+\pi^+$ of (0.14 ± 0.02) %. Several groups have reported observations of a $D^+ \to \phi K^+$ signal, however FOCUS did not find evidence for such decay [16].
SELEX announced the first observation of a Cabibbo suppressed decay of a charm baryon through the decay $\Xi_c^+ \to pK^-\pi^+$ [17]. Fig. 11 shows the signal of 157 ± 22 events reported by SELEX and simple spectator diagrams with external W emission for Ξ_c^+ decaying into a Cabibbo allowed and into a single Cabibbo suppressed (SCS) mode. The other Cabibbo allowed Ξ^- mode interchanges s and d quarks lines and produces a $d\bar{d}$ pair from the vacuum instead of a $d\bar{u}$ pair. FOCUS has also observed the same SCS decay, reporting a signal of 86 ± 21 events from about 70 % of their data.

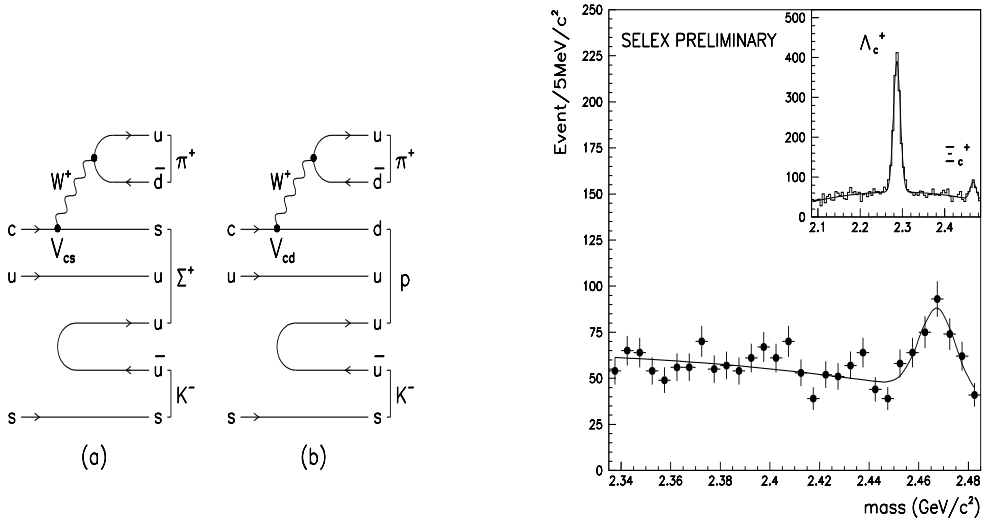

FIGURE 11. Simple spectator diagrams (a) and (b) and preliminary signal of $\Xi_c^+ \to pK^-\pi^+$ from SELEX.

E791 has published [18] results on the singly Cabibbo suppressed decay, $D^0 \to K^-K^+\pi^-\pi^+$. A coherent amplitude analysis of the resonant substructure was used to extract decay fractions. Significant phase angles among different modes

TABLE 2. Branching fractions relative to $D^0 \to K^-\pi^+\pi^-\pi^+$ from E791.

Mode	Branching Fraction
$\phi\rho^0$	$(2.0 \pm 0.9 \pm 0.8)$ %
$\phi\pi^+\pi^-$	$(0.9 \pm 0.4 \pm 0.5)$ %
$\overline{K^{*0}}K^{*0}$	$< 2.0\,\%\,(90\,\%\,CL)$
$\overline{K^{*0}}K^+\pi^- + \overline{K^{*0}}K^-\pi^+$	$< 2.0\,\%\ (90\,\%\,CL)$

indicate very strong interference. The measured branching fractions relative to $D^0 \to K^-\pi^+\pi^-\pi^+$ are presented in the table 2.

Hadronic charm decays, Dalitz plot Analysis

With the advent of high statistics experiments, charm meson decay have become a new way to study light meson spectroscopy. The amplitude analysis performed on Dalitz plots gives insight into the decay dynamics, providing direct information about intermediate resonances and relative decay fractions, and allowing to study final state interactions coming from the interference of the amplitudes describing competing resonant channels.

E791 has preliminary results on the decay of D^+ and D_s^+ mesons in three pions. A clear signal with 1240 ± 51 D^+ and 858 ± 49 D_s^+ was obtained after applying selection criteria aimed at identifying a clearly separated 3π vertex and after carefully estimating the backgrounds coming from possible reflections and three pion combinations. The branching ratios were normalized to $D^+ \to K^-\pi^+\pi^+$ $(34,790 \pm 232$ events) and to $D_s^+ \to \phi\pi^+$ $(1038 \pm 44$ events) respectively. Efficiencies were obtained from a full Monte Carlo simulation. The branching ratio of the $D^+ \to \pi^+\pi^-\pi^+$ relative to $D^+ \to K^-\pi^+\pi^+$ obtained was $0.0329 \pm 0.0015^{+0.0016}_{-0.0026}$. Similarly the branching ratio of the $D_s^+ \to \pi^+\pi^-\pi^-$ relative to $D_s^+ \to \phi\pi^+$ was $0.247 \pm 0.028^{+0.019}_{-0.012}$.

D_s^+ Dalitz plot results from E791

Among the advantages of using charm meson decays to study light I=J=0 states is the fact that, unlike hadron-hadron scattering, in the decays of D mesons the initial state is always $J^P = 0^-$, limiting the number of possible final states. The decay $D_s^+ \to \pi^-\pi^+\pi^+$ is Cabibbo-favored without a strange meson in the final state. It can proceed via spectator amplitudes producing intermediate resonant states with hidden strangeness like the $f_0(980)$ or it can proceed via W-annihilation amplitudes producing intermediate resonant states with no strangeness. The decays like $D_s^+ \to \rho^0\pi^+$ and the non-resonant $D_s^+ \to \pi^-\pi^+\pi^+$ would proceed via W-annihilation mechanism. It would also be responsible for the decay $D_s^+ \to f_0(1370)\pi^+$, if the $f_0(1370)$ resonance is at least partially a $u\bar{u} + d\bar{d}$

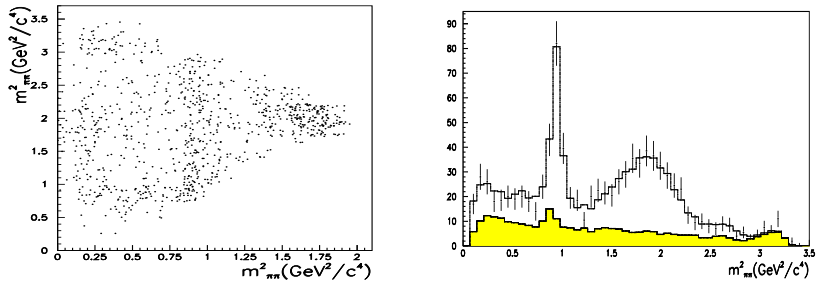

FIGURE 12. The $D_s^+ \to \pi^+\pi^-\pi^+$ Dalitz plot and its projections (preliminary results) from E791.

TABLE 3. Preliminary results of f_0 mass and width of $D_s^+ \to f_0(980)\pi^+$ and $D_s^+ \to f_0(1370)\pi^+$ from E791.

	$f_0(980)$		$f_0(1370)$	
	Mass (MeV/c^2)	width (MeV/c^2)	Mass (MeV/c^2)	width(MeV/c^2)
E791	978 ± 4	44 ± 5	1440 ± 19	165 ± 29
PDG	978 ± 10	$40 - 100$	$1200 - 1500$	$200 - 500$

state as predicted by the simple quark model. The scale of the W-annihilation compared to the W-radiation amplitude would be indicated by the relative contribution of these channels to the $\pi^-\pi^+\pi^+$ final state [19].

The Dalitz plot of $D_s^+ \to \pi^-\pi^+\pi^+$ and the $\pi\pi$ mass projections [20] are shown in Fig. 12.

The $f_0(980)\pi^\pm$ mode is the dominant one, accounting for nearly half of the $D_s^+ \to \pi^-\pi^+\pi^+$ decay width. The $f_0(980)\pi^\pm$ is often supposed to have a large $s\bar{s}$ component, indicating a large spectator amplitude in this decay. Significant contributions of $f_0(1370)\pi^+$ and $f_2(1270)\pi^+$ components were also found. The contribution of $\rho^0(770)\pi^+$ and $\rho^0(1450)\pi^+$ components correspond to about 10 % of the $\pi^-\pi^+\pi^+$ width. This could indicate either contribution from the annihilation diagram or from inelastic final state interactions. No significant non-resonant component was found.
Preliminary f_0 masses and widths [20] from E791 and PDG are presented in the table 3.

FOCUS also has preliminary results of this decay mode. Their preliminary Dalitz plot shows the $D_s^+ \to \pi^-\pi^+\pi^+$ based on a very clean signal of $\sim$ 1300 events reconstructed from 100 % of their data. The preliminary results indicate a negligible contribution from the ρ suggesting negligible Weak Annihilation contribution [21].

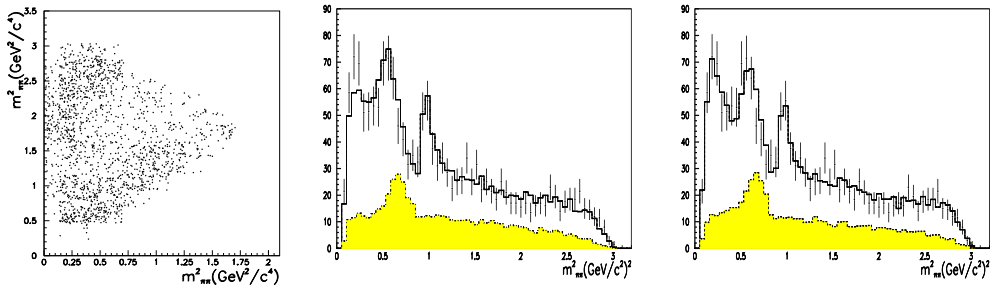

FIGURE 13. $D^+\pi^+\pi^-\pi^+$ Dalitz plot and its projections. The central plot is without a $\sigma\pi$ state and the last plot include a $\sigma\pi$ state in the fit (preliminary results). The shaded area is the background distribution.

D^+ Dalitz plot results and evidence for a light scalar resonance

The Dalitz plot of the single Cabibbo-suppressed decay $D^+ \to \pi^-\pi^+\pi^+$ from E791 data is shown in Fig.13 (left). A coherent amplitude analysis was used to determine the structure of its density distribution. The fit including a non resonant amplitude and amplitudes for D^+ decaying to a π^+ and any of the five established $\pi^+\pi^-$ resonances $\rho^0(770)$, $f_0(980)$, $f_2(1270)$, $f_0(1370)$, and $\rho^0(1450)$ is shown in Fig. 13 (central). This fit is poor in the low $\pi^+\pi^-$ region and has several unsatisfactory features [22]: the NR channel dominates, different from the D_s^+ decay, and the $\rho^0(1450)\pi^+$ is more significant than the $\rho^0(770)\pi^+$ state.

It was found that allowing an additional scalar state, with mass and width unconstrained improves the fit substantially. The mass of the resonance found by this fit is 486^{+28}_{-26} MeV/c^2 and the width 351^{+51}_{-43} MeV/c^2. Referring to this $\pi^+\pi^-$ resonance as the $\sigma(500)$, it was found that $D^+ \to \sigma(500)\pi^+$ accounts for about half of the total decay rate, non-resonant decay was very small and the $\rho^0(1450)\pi^+$ fraction was much less than $\rho^0(770)\pi^+$. Preliminary results of the fit with this state are shown in Fig. 13 (right side).

Theoretically, light scalar and isoscalar resonances are predicted in models for spontaneous breaking of chiral symmetry, like the σ linear model [23]. These scalar particles have important consequences for the quark model, for understanding low energy $\pi\pi$ interactions and also for understanding the $\Delta I = 1/2$ rule.

Multidimensional analysis of $\Lambda_c^+ \to pK^-\pi^+$ from E791

E791 has reported recently the first amplitude analysis of the decay of a charm baryon [24,16]. The study of charm baryon decays can give information regarding

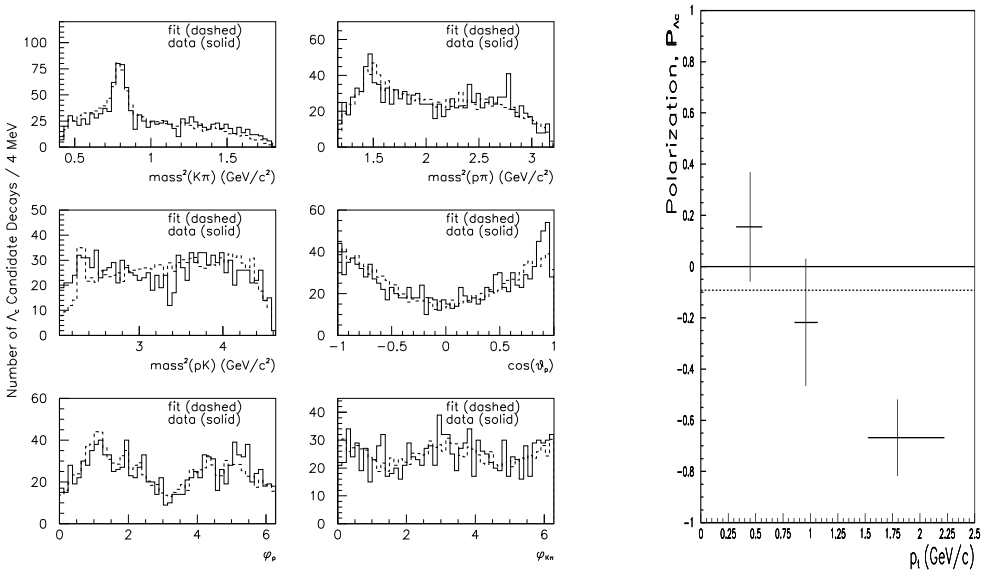

FIGURE 14. Λ_c^+ multidimensional analysis from E791: left plots shows projections of two body masses and angles. Solid line histograms are data in the range $2265 < M_{pK^-\pi^+} < 2315\,\mathrm{MeV/c^2}$. Dashed lines represent the fit in the same range. The right figure shows polarization $P_{\Lambda_c^+}$ vs. p_t.

the relative importance of spectator and exchange amplitudes. Exchange amplitudes are small in charm meson decays because of helicity suppression. However in charm baryon decays this effect should not inhibit exchange amplitudes due to be three body nature of the interaction. The spectator and W-exchange diagrams can contribute to $pK^{*0}(890)$, $\Lambda(1520)\pi^+$ or $pK^-\pi^+$ modes. However for the $\Delta^{++}(1232)K^-$ the W-exchange is the only diagram possible.

The charm baryon can be produced polarized and its decay products carry spin. These extra quantum numbers require five kinematic variables for a complete description of the decay, and instead of the conventional two dimensional Dalitz plot analysis, a five-dimensional amplitude analysis is required.

A sample of 946 ± 38 $\Lambda_c^+ \to pK^-\pi^+$ reconstructed decays was used by E791 to determine relative strengths and phases of resonances in the final state as well as the Λ_c production polarization. The fit projections and the polarization as function of p_t are shown in Fig.14. The resonant fractions for $\Lambda_c^+ \to pK^-\pi^+$ are shown in table 4.

The $\Delta^{++}(1232)K^-$ and the $\Lambda(1520)\pi^+$ decay modes are seen as statistically significant for the first time. The observation of a substantial $\Delta^{++}(1232)K^-$ component provides strong evidence for the W-exchange amplitude in charm baryon decays. It was also observed an increasingly negative polarization for the Λ_c as a function of p_t.

TABLE 4. Resonant fractions for Λ_c^+ decay modes.

Decay Mode	% of $pK^-\pi^+$
$pK^{*0}(890)$	$19.5 \pm 2.6 \pm 1.8$
$\Delta^{++}(1232)K^-$	$18.0 \pm 2.9 \pm 2.9$
$\Lambda(1520)\pi^+$	$7.7 \pm 1.8 \pm 1.1$
non-resonant	$54.8 \pm 5.5 \pm 3.5$

RARE AND FORBIDDEN DECAYS

In the charm sector the rare and forbidden dilepton decay modes can be classified mainly into three categories (example of Feynman diagrams are shown in Fig. 15):
1) Flavor Changing Neutral Current decays (FCNC) such as $D^0 \to l^+l^-$ and $D^+ \to h^+l^+l^-$.
2) Lepton Family Number Violating decays (LFNV) such as $D^+ \to h^+l_1^+l_2^-$ and $D^0 \to l_1^+l_2^-$ where the leptons are from different generations.
3) Lepton number Violating decays (LNV) such as $D^+ \to h^-l^+l^+$ where the leptons are of the same generation but have the same sign.
Where h stands for π, K and l for e, μ.
The first decay modes (FCNC) are rare, that means a process suppressed via the GIM mechanism which proceeds via an internal quarks loop in the Standard Model [25]. The FCNC decay mode $D^0 \to l^+l^-$ can proceed via a W box diagram and the theoretical estimates [26] for the branching fraction are of the order of $\sim 10^{-19}$. The predictions for the other FCNC decay modes, $D^+ \to h^+l^+l^-$, are considerably larger, of the order of $\sim 10^{-9}$. These decay modes can proceed via penguin diagrams [25] and from long distance effects.
The decays modes LFNV and LNV are strictly forbidden in the Standard Model as they do not conserve lepton number. However, some theoretical extensions of the Standard Model predict lepton number violation [27], and then the observation of a signal in these modes would be evidence for new physics beyond the SM.

E791 has recently published [28] (see figure 15) a set of new limits in rare or forbidden decay modes that improve the PDG98 numbers by a factor of 10. They searched for 24 different rare and forbidden decay modes and have found no evidence for them. They therefore presented upper limits on their branching fractions. Fourteen of their limits represent a significant improvement over previous results and eight are presented for the first time.

For this study E791 used a *blind* analysis technique. The mass region where the signal is expected is *masked* throughout the analysis. Selection criteria are optimised by studying signal events generated by Monte Carlo simulation and background events obtained from data in mass windows above and below the *signal region*. The criteria were chosen to maximize the ratio $N_S/\sqrt{(N_B)}$, where N_S and N_B are the numbers of signal and background events, respectively. Only after this

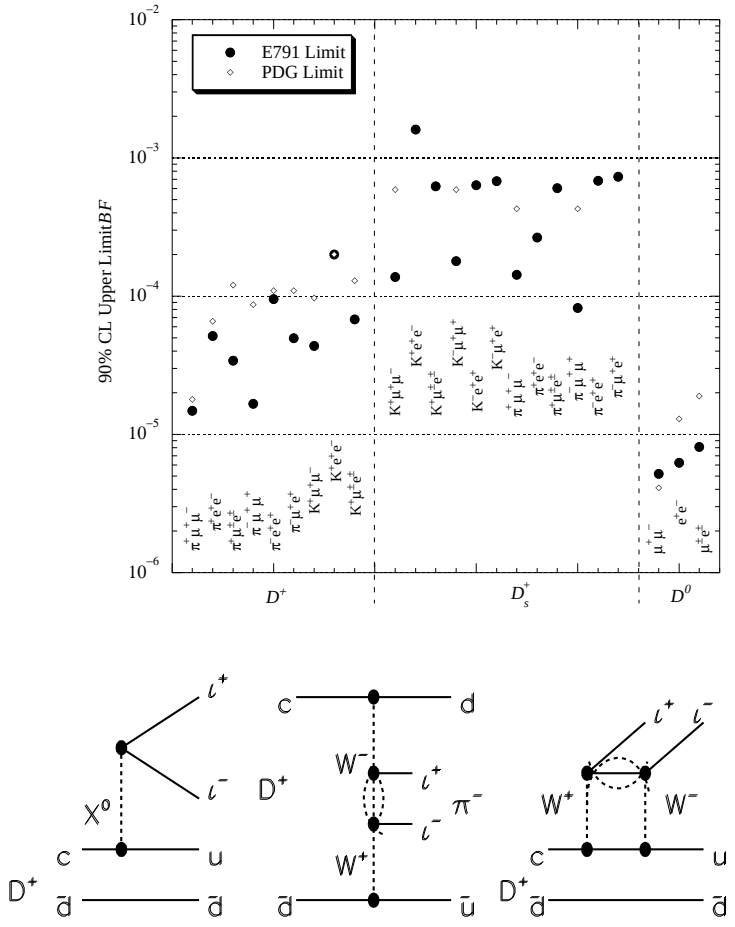

FIGURE 15. Rare decays limits from E791 (top) and some Feynman diagrams for FCNC, LFNV and LNV decay modes (bottom).

procedure were events within the signal window unmasked. This blind technique is used so that the presence or absence of signal does not bias the choice of the selection criteria.

FOCUS is also looking for rare and forbidden decays using the same technique. Some examples of rare decays are presented in table 5 where we compare the expected sensitivity from FOCUS to E791 results and PDG values.

TABLE 5. Rare decays limits from FOCUS (preliminary), E791 and PDG98.

Decay mode	FOCUS expected sensitivity (45 % of the data)	E791[a] 90 % C.L. limit	PDG 98 90 % C.L limit
$D^+ \to K^+\mu^+\mu^-$	8.1×10^{-6}	4.4×10^{-5}	9.7×10^{-5}
$D^+ \to K^-\mu^+\mu^+$	12.1×10^{-6}		1.2×10^{-4}
$D^+ \to \pi^+\mu^+\mu^-$	7.8×10^{-6}	1.5×10^{-5}	1.8×10^{-5}
$D^+ \to \pi^-\mu^+\mu^+$	7.1×10^{-6}	1.7×10^{-5}	8.7×10^{-5}
$D^+ \to \mu^-\mu^+\mu^+$	4.4×10^{-6}		

[a] Published [28]

SEMILEPTONIC DECAYS, FORM-FACTORS

The weak decays of hadrons containing heavy quarks are influenced by strong interaction effects. Semileptonic charm decays such as $D^+ \to \overline{K}^{*0} e^+ \nu_e$, $D_s^+ \to \phi l^+ \nu_l$ are an especially clean way to study these effects because the leptonic and hadronic currents completely factorize in the decay amplitude ,A, as we can see in the Eq. 4, where G_F is the Fermi coupling constant for the weak interaction and V_{cs} is the CKM matrix element. L^μ (Eq. 5) and H_μ (Eq. 6) represent the leptonic and hadronic currents [29].

$$A(D^+ \to \overline{K^*}^0 e^+ \nu_e) = \frac{G_F}{\sqrt{2}} V_{cs} L^\mu H_\mu \tag{4}$$

$$L^\mu = \bar{u}_e \gamma^\mu (1 - \gamma_5) v_\nu \tag{5}$$

$$H_\mu = (m_D + m_{K^*}) A_1(q^2) \epsilon_{mu} - \frac{A_2(q^2)}{m_D + m_{K^*}} (\epsilon \cdot p_D)(p_D + p_K)_\mu - \frac{A_3(q^2)}{m_D + m_{K^*}} (\epsilon \cdot p_D)(p_D - p_K)_\mu - i \frac{2V(q^2)}{m_D + m_{K^*}} \varepsilon_{\mu\nu\rho\sigma} \epsilon^\nu p_D^\rho p_K^\sigma \tag{6}$$

With a vector meson in the final state, there are four form factors, $V(q^2)$, $A_1(q^2)$, $A_2(q^2)$ and $A_3(q^2)$, which are functions of the Lorentz-invariant momentum transfer squared q^2, the square of the invariant mass of the virtual W [29]. The differential decay rate for $D^+ \to \overline{K}^{\star 0} \mu^+ \nu_\mu$ with $\overline{K}^{\star 0} \to K^- \pi^+$ is a quadratic homogeneous function of the four form factors. Unfortunately, the limited size of current data samples does not allow precise measurement of the q^2-dependence of the form factors; we thus assume the dependence to be given by the nearest-pole dominance model: $F(q^2) = F(0)/(1 - q^2/m_{pole}^2)$ where $m_{pole} = m_V = 2.1\ \mathrm{GeV}/c^2$ for the vector form factor V (which correspond to $J^P = 1^+$ state, D_{s1}^*), and $m_{pole} = m_A = 2.5\ \mathrm{GeV}/c^2$ for the three axial- vector form factors A [30] (corresponding to 1^- state, D_s^*).

The third form factor $A_3(q^2)$, which is unobservable in the limit of vanishing lepton mass, probes the spin-0 component of the off-shell W. Additional spin-flip amplitudes, suppressed by an overall factor of m_ℓ^2/q^2 when compared with spin no-flip amplitudes, contribute to the differential decay rate. Because $A_1(q^2)$ appears among the coefficients of every term in the differential decay rate, we can factor out $A_1(0)$ and measure the ratios:
$r_V = V(0)/A_1(0)$, $r_2 = A_2(0)/A_1(0)$ and $r_3 = A_3(0)/A_1(0)$. The values of these ratios can be extracted without any assumption about the total decay rate or the weak mixing matrix element V_{cs}.

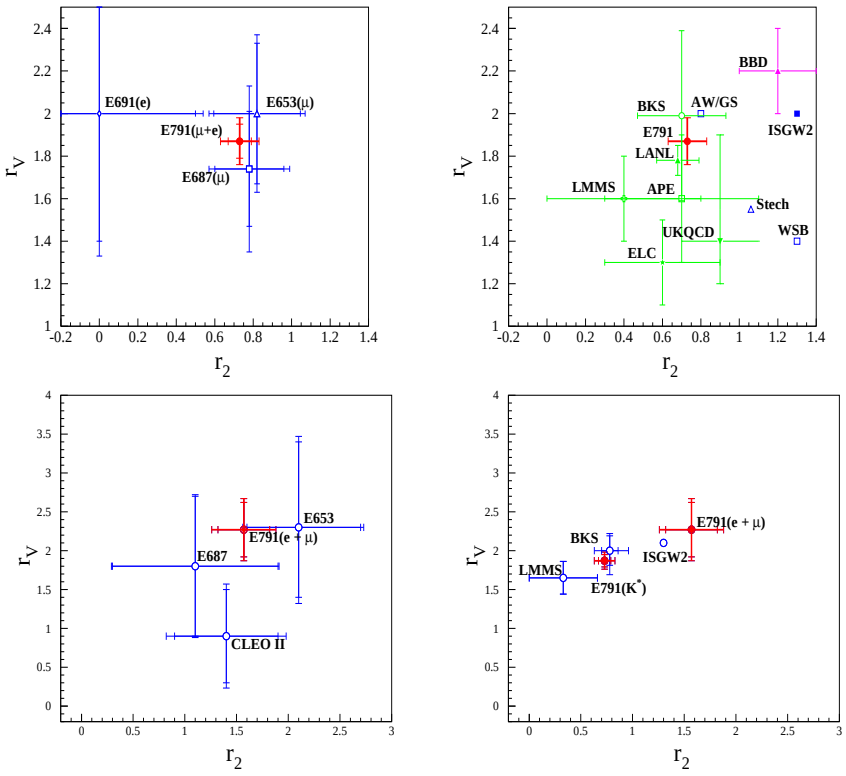

FIGURE 16. Top-left figure present the ratios r_2 and r_V for $D^+ \to \overline{K^{*0}} l\nu_l$, and top-right compare them to theoretical models. Bottom-left show ratios r_2 and r_V for $D_s^+ \to \overline{\phi} l\nu_l$, and bottom-right is a comparison with theoretical models.

We report E791 measurements of the form factor ratios r_v and r_2 for the muon channel [31] and combined with electron channel [32] (see Fig. 16). This is the first set of measurements in both muon and electron channels from a single experiment. We also report the first measurement of $r_3 = A_3(0)/A_1(0)$, which is unobservable in the limit of vanishing charged lepton mass.

The measurements of the form factor ratios for $D^+ \to \overline{K}^{\star 0}\mu^+\nu_\mu$ presented here and for the similar decay channel $D^+ \to \overline{K}^{\star 0}e^+\nu_e$ [33] follow the same analysis procedure except for the charged lepton identification. Both results in the electron and muon channels are consistent within errors, supporting the assumption that strong interaction effects incorporated in the values of form factor ratios do not depend on the particular W^+ leptonic decay.
The combined results of electronic and muonic decay modes produce $r_V = 1.87 \pm 0.08 \pm 0.07$ and $r_2 = 0.73 \pm 0.06 \pm 0.08$. The combination of all systematic errors is ultimately close to that which one would obtain assuming all the errors are uncorrelated. The third form factor ratio $r_3 = 0.04 \pm 0.33 \pm 0.29$ was not measured in the electronic mode.
Table 6 compares the values of the form factor ratios r_V and r_2 measured by E791 in the electron, muon and combined modes with previous experimental results. The size of the data sample and the decay channel are listed for each case. All experimental results are consistent within errors. The comparison between the E791 combined values of the form factor ratios r_V and r_2 and other experimental results is also shown in Fig. 16 together with theoretical predictions.

TABLE 6. Comparison of E791 results with previous results.

Exp.	Events	$r_V = V(0)/A_1(0)$	$r_2 = A_2(0)/A_1(0)$
E791	6000 $(e+\mu)$	$1.87 \pm 0.08 \pm 0.07$	$0.73 \pm 0.06 \pm 0.08$
E791	3000 (μ)	$1.84 \pm 0.11 \pm 0.09$	$0.75 \pm 0.08 \pm 0.09$
E791	3000 (e)	$1.90 \pm 0.11 \pm 0.09$	$0.71 \pm 0.08 \pm 0.09$
E687 [35]	900 (μ)	$1.74 \pm 0.27 \pm 0.28$	$0.78 \pm 0.18 \pm 0.10$
E653 [36]	300 (μ)	$2.00^{+0.34}_{-0.32} \pm 0.16$	$0.82^{+0.22}_{-0.23} \pm 0.11$
E691 [37]	200 (e)	$2.0 \pm 0.6 \pm 0.3$	$0.0 \pm 0.5 \pm 0.2$

The FOCUS experiments anticipate measuring r_2 and r_V to better precision than previous experiments [34]

CHARM LIFETIMES

The study of the charm particle lifetimes is motivated by two main goals: to extract partial decay rates and to study decay dynamics. The total decay width can be expressed as a sum of the three possible classes of decays, so the lifetime of a particle can be written as

$$\tau = \frac{\hbar}{\Gamma_{tot}} = \frac{\hbar}{\Gamma_{leptonic} + \Gamma_{SL} + \Gamma_{nonleptonic}} \tag{7}$$

The leptonic partial width is normally very small ($\Gamma_{leptonic} \sim 10^{-3} - 10^{-4}$) due to helicity suppression. The observed $\Gamma_{SL}(D^+)$ and $\Gamma_{SL}(D^0)$ are equal to within 10%,

as expected from isospin invariance. So, the large difference observed in the D^+ and D^0 lifetimes, $\tau(D^+)/\tau(D^0) = 2.55 \pm 0.04$, is due to a large difference in the hadronic decay rates ($\Gamma_{nonleptonic}$) for the D^+ and the D^0. If there were no other diagram but the spectator and no QCD effects we would have the same value for τ. Thus, the different lifetimes are an indication that we need to take into account contributions from diagrams where the W interact with two valence quarks, such as W-annihilation (WA) and W-exchange (WX), and any interference between them, as shows the Fig. 17.

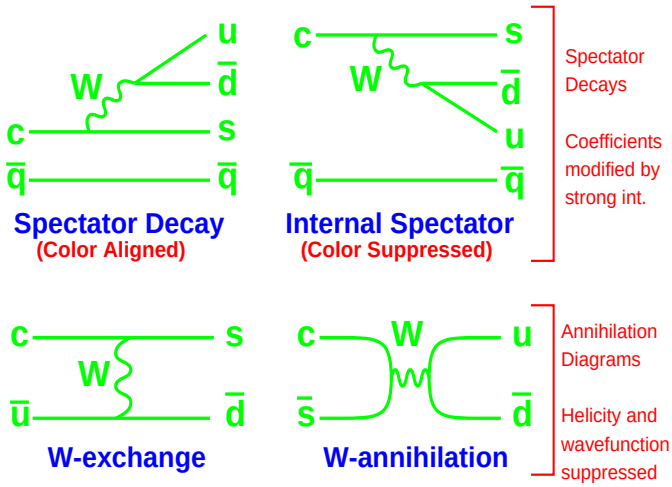

FIGURE 17. Hadronic decays diagrams for charm meson decays.

A systematic approach now exists for the treatment of inclusive decays, based on QCD and consists of an Operator Product Expansion (OPE) in the Heavy Quark mass. In this approach the interaction is factorized into three parts: weak interaction between quarks, perturbative QCD corrections and non-perturbative QCD effects. The decay rate is given by

$$\Gamma_{HQ} = \frac{G_F^2 m_Q^2}{192\pi^3} \Sigma f_i |V_{Qq_i}|^2 [A_1 + \frac{A_2}{\Delta^2} + \frac{A_3}{\Delta^3} + \ldots] \tag{8}$$

where Δ is taken as the heavy quark mass and f_i is a phase space factor. $A_1 = 1$ contains the spectator diagram contribution; A_2 is the spin interaction of the heavy quark with light quark degrees of freedom inside the hadron and produces differences between the baryon and meson lifetimes; A_3 includes the non-spectator W-annihilation, W-exchange and Pauli Interference (PI) of the decay and the spectator quarks contributions.

New results on charm lifetime measurements are shown in table 7. The most relevant information is the D_s^+ lifetime from E791 [38,39] and FOCUS [40] which is now conclusively above the D^0 lifetime, with a ratio

$$R_\tau = \tau(D_s^+)/\tau(D^0) = 1.22 \pm 0.02 \tag{9}$$

It is important to note that R_τ is now ten standard deviations away from unity, indicating that although not dominant, the WA/WX contributions are significant. In fact the OPE model predicts R_τ = 1.00 - 1.07 without WA/WX contributions, allowing a variation of $\pm 20\%$ if the WA/WX operators are included, in agreement with the new result.

In the baryon sector SELEX and FOCUS have preliminary measurements of the Λ_c^+ lifetime, as shown in table.7 and Fig. 18. Using 100% of their data in $\Lambda_c^+ \to pK^-\pi^+$, SELEX find $\tau = 177 \pm 10(stat) fs$ [41], in a $2-3\sigma$ disagreement with PDG98 and FOCUS.

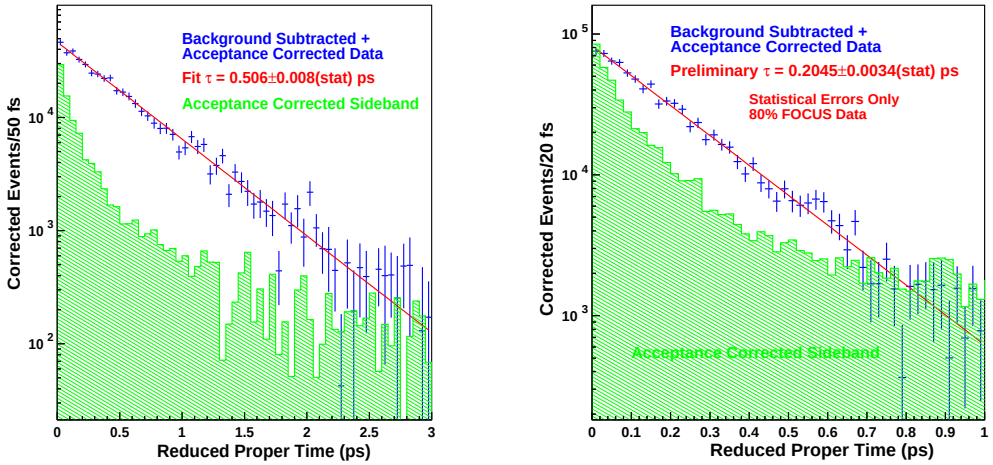

FIGURE 18. D_s^+ (left) and Λ_c^+ (right) lifetimes from FOCUS (preliminary results)

TABLE 7. Summary of new charm lifetime measurements.

Experiment	$\tau(D^+)$ fs	$\tau(D^0)$ fs	$\tau(D_s^+)$ fs	$\tau(\Lambda_c^+)$ fs
PDG'98	1057 ± 15	415 ± 4	467 ± 17	206 ± 12
E791[a]	1065 ± 48	$413 \pm 3 \pm 4$	$518 \pm 14 \pm 7$	
CLEO	$1033.6 \pm 22.1^{+9.9}_{-12.7}$	$408 \pm 4.1^{+3.5}_{-3.4}$	$486.3 \pm 15.0^{+4.9}_{-5.1}$	
FOCUS[b]			506 ± 8	204.5 ± 3.4
SELEX[b]				177 ± 10
World Average	1052 ± 12	412.8 ± 2.7	499.9 ± 6.1	201.9 ± 3.1

[a] $\tau(D^+)$ using only the $\phi\pi^+$ mode.
[b] Preliminary results with no systematic uncertainty quoted

Lifetime differences and $D^0\overline{D^0}$ mixing

E791 has published searches for a lifetime difference between the $CP-even$ and $CP-odd$ eigenstates of the D^0 [39]. To do so they compared the lifetimes of the decays $D^0 \to K^-K^+$ $(CP=+1)$ and $D^0 \to K^-\pi^+$, (CP mixed) [42], shown in Fig. 19.

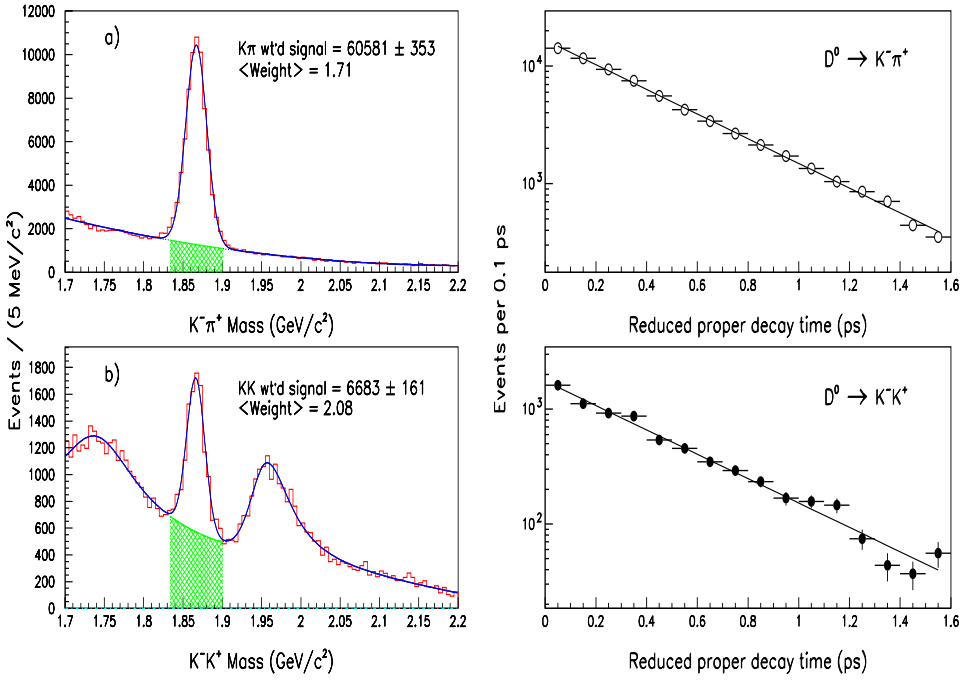

FIGURE 19. Invariant mass for $D^0 \to K^-\pi^+$ (a) and $D^0 \to K^-K^+$ (b) decays (left). Exponential fits for number of decays as a function of reduced proper decay time (right), (E791 results).

Defining

$$\frac{\Gamma(K^-K^+)-\Gamma(K^-\pi^+)}{\Gamma(K^-\pi^+)} = y_{CP} \tag{10}$$

The time integrated ratio of mixed to non mixed decay rates in charm meson is given by

$$R_{mix} = \frac{\Gamma(D^0 \to \overline{D^0} \to \bar{f})}{D^0 \to f} = \frac{x^2+y^2}{2} \tag{11}$$

where

$$x = \frac{\Delta m}{\overline{\Gamma}}, \quad y = \frac{\Delta\Gamma}{2\overline{\Gamma}}$$

with

$$\Delta m = m_1 - m_2, \quad \Delta\Gamma = \Gamma_1 - \Gamma_2, \quad \overline{\Gamma} = (\Gamma_1 + \Gamma_2)/2$$

where Γ_1 is for CP even states and Γ_2 for CP-odd states.
Γ_1 applies to $D^0 \to K^-K^+$ and Γ applies to $D^0 \to K^-\pi^+$ if CP is conserved.
Mixing can appear if there is either a difference in the masses of the CP eigenstates Δm or if there is a difference in the decay rates $\Delta\Gamma$.

E791 observed no difference in lifetimes and quoted $\tau(K\pi) = 0.413 \pm 0.003 \pm 0.004$ ps $\tau(KK) = 0.410 \pm 0.011 \pm 0.006$ ps, $y_{CP} = 0.008 \pm 0.029 \pm 0.010$ or $-0.04 < y_{CP} < 0.06$ (90% CL) or $\Delta\Gamma = 2(\Gamma_{KK} - \Gamma_{K\pi}) = (0.04 \pm 0.14 \pm 0.05)\, ps^{-1}$

ACKNOWLEDGEMENTS

One of us, J. C. Anjos would like to thank the conference organizers for their invitation to attend the Symposium. E. Cuautle would like to thank the Centro Brasileiro de Pesquisas Físicas (CBPF) for its kind hospitality during his postdoctoral stay. The authors would like to thank CLAF/CNPq (Brazil) and CONACyT (México) for financial support of this work.

REFERENCES

1. Nason, P., Dason, S., Ellis, R. K., *Nucl. Phys.* **303 B**, 607 (1998).
2. Mangano, M., Nason, P., and Ridolfi, G., *Nucl. Phys.* **B 373**, 295 (1992).
   Frixione, S., Mangano, M., Nason, P., and Ridolfi, G., *Nucl. Phys.* **B 431**, 453 (1994).
3. Sjöstrang, T., Pythia 7.5 and Jetset 7.4 Manual, CERN-TH 71112/93, 1995.
4. Aitala, E. M., et al., *Fermilab E791 Collaboration*, *Phys. Lett.* **462 B**,225 (1999).
5. Aguilar-Benitez, M., et al., *CERN LEBC-EHS Collaboration*, *Phys. Lett.* **164B**, 404 (1985);
   Aguilar-Benitez, M., et al., *CERN LEBC-EHS Collaboration*, *Z. Phys.* **C40**, 321 (1988); Aoki , S. , et al., *Phys. Lett.* **209 B**,113 (1988); Kodama, K., et al., *Phys. Lett.* **263 B**, 579 (1991); Berlag, S. et al., *ACCMOR Collaboration*, *Phys. Lett* **257 B**, 519 (1991).
6. Appel, J.A., *Annu. Rev. Nucl. Part.Sci.* **42**, 367 (1992).
7. Aitala, E. M., et al., *Fermilab E791 Collaboration*, *Eur. Phys. J.* **C4**, 1 (1999)
8. Sjöstrand, T., *International Journal of Mod. Phy.* **A 3**, 751 (1988).
9. Brodsky, S.J., et al.,*Phys. Lett.* **93 B** , 451(1980).
10. Iori M., et al., *Fermilab SELEX Collaboration*, *Charm hadroproduction results from SELEX*, hep-ex/99100039.

García, F.G., *Fermilab SELEX Collaboration*, *Charm hadroproduction from SELEX*, *Wine and Cheese Seminar, Fermilab Aug. 99*
11. Anjos, J.C. *Particle-antiparticle asymmetries in the production of baryons in 500 GeV/c π^-- Nucleon interactions*, (to appear, Proc.) Hyperon Physics Symposium (HYPERON 99), Fermilab, Sept. 99. Preprint hep-exp/9912039.
12. Aitala, E. M., et al., *Fermilab E791 Collaboration*, *Phys. Lett.* **411 B**, 230 (1997)
13. Aitala, E. M., et al., *Fermilab E791 Collaboration*, *Phys. Lett.* **371 B**,157 (1996)
14. Anjos, J.C., et al., *Asymmetry studies in $\Lambda^0/\bar{\Lambda^0}$, Ξ^-/Ξ^+ and Ω^-/Ω^+ production*, *First Tropical Workshop and Second Latin American Symposium*, San Juan, Puerto Rico, 1998. Ed. J.F. Nieves. AIP, Conference Proceedings 444, p. 540.
15. Aitala, E. M., et al., *Fermilab E791 Collaboration*, *Phys. Lett.* **404 B**, 187 (1997).
16. Brian, M., *Experimental Results on hadronic c decays*, (to appear, Proc.) *Heavy Flavours 8*, Southampton, UK. 1999.
17. Jun, S. Y., et al., *Fermilab SELEX Collaboration*, *Observation of the Cabibbo-suppressed decay $\Xi_c^+ \to pK^-\pi^+$*, hep-ex/9907062.
18. Aitala, E. M., et al.,*E791 Collaboration*, *Phys. Lett.* **423B**, 185 (1998).
19. Reis, A., *Light Scalars Through Charm Decays*, (to appear, Proc.) *Physics and detectors for da Φne (DAFNE99)*, Frascati, Nov. 1999.
20. Aitala, E. M., et al., *Fermilab E791 Collaboration*, preprint Fermilab-Pub-99/323-E
21. Moroni, L. *First results from FOCUS*, (to appear, Proc.) *International Europhysics Conference on High Energy Physic 99*, Finland, July 1999
22. Aitala, E. M. et al., *Fermilab E791 Collaboration*, preprint Fermilab-Pub-99/322-E
23. Nambu, Y. and Jona-Lasinio G., *Phys. Rev.* **122**, 345 (1961).
24. Aitala, E. M., et al., *Fermilab E791 Collaboration*, *Phys. Lett.* **471 B**, 449 (2000).
25. Schwartz, A. J., *Mod. Phy. Let.* **A8**, 967 (1993).
Schwartz, A. J., *Recent Charm Results from Fermilab Experiment E791*, preprint hep-ex/9908054.
26. Hewett, J. L., *Heavy Flavor Physics* preprint hep-ph/9505246.
27. Pakvasa, S., *Flavor Changing Neutral Currents in Charm sector* (hep-ph/9705397).
28. Aitala, E. M., et al., *Fermilab E791 Collaboration*, *Phys. Lett.* **462 B**, 401 (1999).
29. Körner, J. G. and Schuler, G. A.,*Phys. Lett.* **B 226**, 185 (1989).
30. Particle Data Group, Review of Particle Physics, *Phys. Rev.* **D 50**, 1568 (1994).
31. Aitala, E. M., et al., *Fermilab Collaboration*, *Phys. Lett.* **450 B**, 294 (1999).
32. Aitala, E. M., et al., *Fermilab Collaboration*, *Phys. Lett.* **440 B** , 435 (1998).
33. Aitala, E. M., et al., *Fermilab E791 Collaboration*, *Phys. Rev. Lett.* **80**, 1293 (1998).
34. Brian O' Reilly, *Charmed Baryon and Semileptonic Physic at FOCUS*, (to appear, Proc.) *III International Conference on Hyperons Charm and Beauty hadrons*, Genova Italy, July 1998.
35. Frabetti, P.L., et al., *Fermilab E687 Collaboration*, *Phys. Lett.* **307 B**, 262 (1993).
36. Kodama, K. et al., *E653 Collaboration*, *Phys. Lett.* **274 B**, 246 (1992)
37. Anjos, J.C., et al., *Fermilab E691 Collaboration*, *Phys. Rev. Lett.* **65**, 2630 (1990).
38. Aitala, E. M., et al., *Fermilab E791 Collaboration*, *Phys. Lett.* **445 B**, 449 (1999).
39. Aitala, E. M., et al., *Fermilab E791 Collaboration*, *Phys. Rev. Lett.* **83**, 32 (1999).
40. Cheung, H.W.K., *FOCUS Collaboration*, *Preliminary D_s^+ lifetime from FOCUS*, APS Centennial Meeting Atlanta March 1999. *Review of Charm Lifetimes*, (to ap-

pear, Proc.) *Heavy Flavours 8*, Southampton, UK. 1999.

41. Kushnirenko, A. Y., *SELEX Collaboration*, *Charm Physics Results from SELEX*, 4th Workshop on Heavy Quarks at Fixed Target, Batavia Illinois, USA, October 1998. Eds. H. W. K. Cheung and J. N. Butler. AIP, Conference Proceedings 459 p. 168.
42. Bianco S., *Charm Overview*, (to appear, Proc.) *Physics in Collision (PIC99)*, Michigan, June 1999 (hep-ex/9911034).
    Appel, J. A., *Charm Results on CP violation and Mixing*, (to appear, Proc.) *Physics and detectors for da Φne (DAFNE99)*, Frascati, Nov. 1999. Sheldon, P.D., *Charm Mixing and Rare Decays*, (to appear, Proc.) *Heavy Flavours 8*, Southampton, UK. 1999.